

Dynamic-Mechanical Study of Water-Blown Rigid Polyurethane Foams with and without Soy Flour

LI-CHUNG CHANG,¹ YU XUE,² FU-HUNG HSIEH²

¹ Aromatic Chemical Industrial Co., Ltd., Tayuan Hsiang, Taoyuan Hsien, Taiwan, Republic of China

² Department of Biological Engineering, University of Missouri–Columbia, Columbia, Missouri 65211

Received 10 January 2000; accepted 2 December 2000

ABSTRACT: Glass transition temperatures of water-blown rigid polyurethane foams at three levels of initial water content, 4.5–5.5%, and five levels of soy flour, 0–40%, were determined by dynamic-mechanical instrumentation at the temperature range of 50–280°C and the frequencies from 0.1 to 20 Hz. The results showed that both the addition of soy flour in the rigid polyurethane foam system and increasing initial water content contributed to a higher glass transition temperature. Moreover, increasing the percentage of the soy flour in the rigid polyurethane foam system led to higher compressive strength and broader master curves for the imaginary part of the elastic modulus. The KWW function fitted the master curve better than the HN and CD functions. © 2001 John Wiley & Sons, Inc. *J Appl Polym Sci* 81: 2027–2035, 2001

Key words: rigid polyurethane foam; dynamic-mechanical properties; glass transition temperature

INTRODUCTION

Polyurethane foams have been commercially developed since the 1940s. These foams are playing an important role in many industries and contribute greatly to our daily lives, such as shipbuilding, footwear, construction, cars, insulation, furniture, car seating, and packaging.¹ They have been at the fifth position in the production volume of plastics.² The use of polyurethane foams is growing at a rapid pace throughout the world.

Polymer blends, such as polyurethane foams with and without biomass, not only have practical value in diverse applications, but also are of great interest in the study of viscoelasticity. As in the case of a pure polymer, an important phenomenon to be considered in the applications of polymer blends is the presence of one or several glass

transitions. These transitions may limit the performance of these materials when they are used over large temperature intervals. As a result, much attention has been devoted to the description of the glass transition of polymeric materials.

The glass transition has been the subject of experimental and theoretical studies for many years.^{3,4} Recent theoretical approaches provide new information on the physical processes responsible for the glass transition and present the glass transition as a dynamic transition.⁵ Two frequently used theoretical approaches are the coupling model and the mode–mode coupling theory (MCT).^{6,7} In both, the calculation of the properties of the system from first principles is not possible because the polymer blends are complex systems. Therefore, the use of fitting parameters is necessary. During the last few years relaxation data are used to test some of the predictions of the MCT (mainly dielectric relaxation).^{7–10} Also, the coupling model describes the relaxation behavior of polymers and blends near the glass transi-

Correspondence to: F.-H. Hsieh.

Journal of Applied Polymer Science, Vol. 81, 2027–2035 (2001)
© 2001 John Wiley & Sons, Inc.

tion.^{11,12} These only applied to the linear polymers or linear polymer blends, but polyurethane foams have a more complicated structure than the linear polymers and linear polymer blends. Furthermore, addition of soy flour in the rigid polyurethane foam system has been reported to increase its compressive strength and dimensional stability during thermal and humid aging.^{13,14} The effect of adding soy flour on the glass transition temperature of the rigid polyurethane foam system has never been reported. The objectives of this study were to determine glass transition temperatures of polyurethane foams with and without soy flour, and the parameters with different temperatures and frequencies, make master curves, and calculate C_1 and C_2 of Williams-Landel-Ferry (WLF), as well as fit master curves using the empirical relaxation functions, such as Kohlrausch-Williams-Watts (KWW), Havriliak-Negami (HN), and Cole-Davidson (CD), for describing relaxation behavior.

EXPERIMENTAL

Materials

The soybean flour used in the preparation of water-blown rigid polyurethane foams was Soyafuff 200W (Central Soya, Fort Wayne, IN). The chemicals included polymeric isocyanate (PAPI 27, Dow Chemical, Midland, MI), polyether polyol (Voranol 490, Dow Chemical, Midland, MI), catalysts (Toyocat-TF and TMF, Tosoh USA, Atlanta, GA), surfactant (L-5440, OSI Specialties, Sistersville, WV), and a blowing agent (distilled water).

Experimental Design and Formulations

The effects of the following variables in the foam formulation on the properties of water-blown rigid polyurethane foams were studied: (1) concentrations of soybean flour (parts per hundred polyols): 0, 10, 20, 30, and 40; and (2) water contents (parts per hundred polyols): 4.5, 5, and 5.5. Other factors in the foam formulation, such as catalysts, surfactant, and isocyanate index, were kept constant. The concentrations of catalysts and surfactant in the foam formulation were determined first to ensure that all foam products can be prepared within the normal amount of time (10 min). This experiment is a 5×3 factorial rearrangement. The foam formulation for water-blown rigid polyurethane foam is in Table I. The amount of isocyanate added in each formulation

Table I Formulations for Water-Blown Rigid Polyurethane Foam

Ingredients	Parts by Weight
Component A	
Polyol ^a	100
Soy flour ^b	0, 10, 20, 30, 40
Catalysts ^c	2.5 & 2.5
Surfactant ^d	3.0–4.0
Blowing agent (distilled water)	4.5, 5.0, 5.5
Component B	
Polymeric MDI ^e	225, 234, 243

^a Polyether polyol (Voranol 490, Dow Chemical, Midland, MI).

^b Defatted soy flour (Soyafuff 200 W, Central Soya, Fort Wayne, IN).

^c Toyocat-TF and TMF (Tosoh USA, Atlanta, GA).

^d Surfactant (L-5440, OSI Specialties, Sistersville, WV).

^e Polymeric isocyanate (PAPI 27, Dow Chemical, Midland, MI). The quantity of isocyanate is based on an isocyanate index 120, defined as the actual amount of isocyanate used over the theoretical amount of isocyanate required, multiplied by 100.

was based on total hydroxyl content of the polyether polyol and water. Three replicate foams were produced with each formulation.

Foam Preparation

A standard laboratory mixing and pouring procedure for making foams was used.¹⁵ Intensive mixing was generated by a commercial drill press (Buffalo, Colcord-Wright, St. Louis, MO) with a 25.4-cm shaft and a 5-cm impeller. Soybean flours were dried in a vacuum oven at 70°C and 50 mmHg overnight. Polyether polyol, catalysts, soybean flour, surfactant, and blowing agent (component A) were added by weight into a 1-quart disposable paperboard container holding a steel frame with four baffles next to the container wall and mixed at 3450 rpm for 60–120 s. Then stirring was stopped, allowing the mix to degas. After 15 s, polymeric isocyanate (component B) was rapidly added, and stirring was continued for another 15–25 s at the same speed. The reacting mixtures were then poured immediately into wooden boxes (20 × 20 × 10 cm) and allowed to rise at ambient conditions. Foams were removed from boxes after 1 h and cured at room conditions (23°C) for 1 week before dynamic-mechanical measurements.

Dynamic-Mechanical Measurements

The dynamic-mechanical properties were obtained using a Dynamic Mechanical Spectrometer 6100

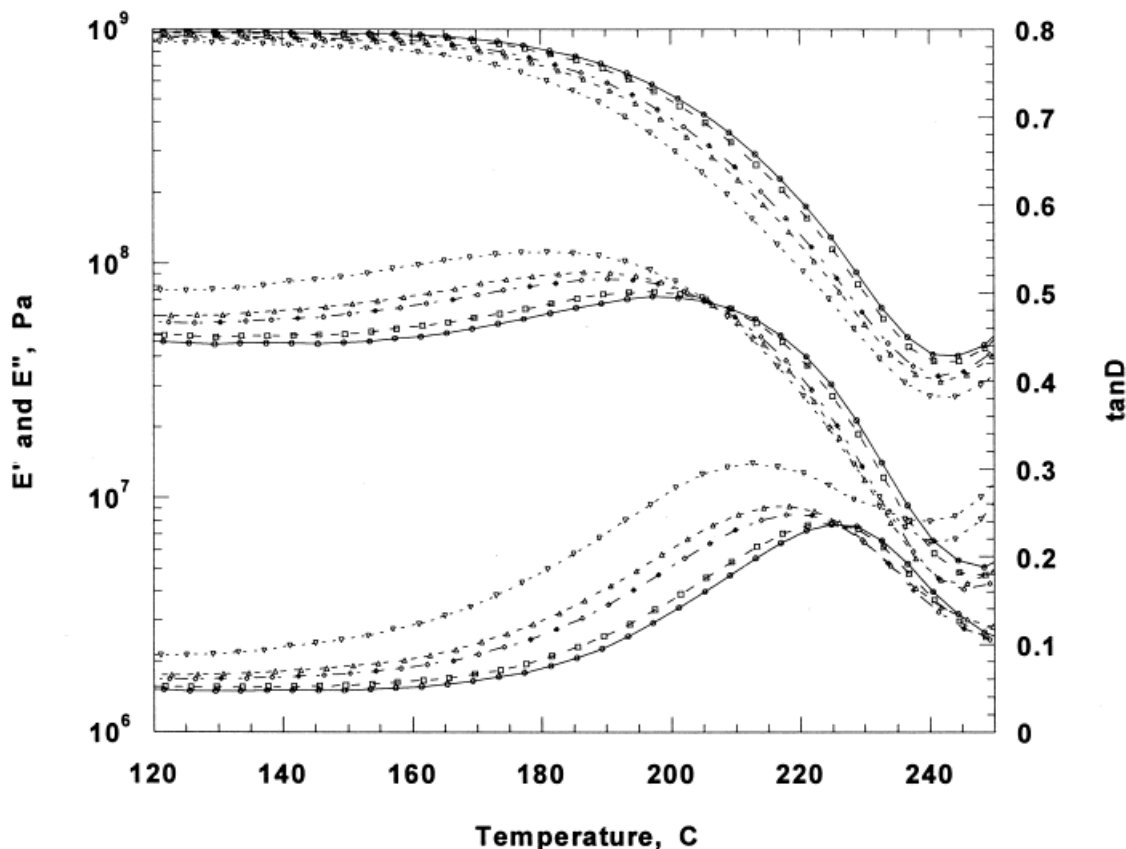


Figure 1 E' , E'' , and $\tan \delta$ of the control foam at 4.5% initial water content. Symbols correspond to experimental data at frequencies of 10 (O), 5 (□), 1 (◇), 0.5 (△), and 0.1 (▽) Hz.

(DMS 6100) (Seiko Instruments, Koto-ku, Japan) in the compression mode. The approximate cylindrical dimension of the foam samples used was 10.0 mm (D) \times 10.0 mm (H). Samples were heated at a rate of 2°C/min over the range of 50–280°C. The sinusoidal oscillation measurement was at the frequencies from 0.1 to 20 Hz and at a compression of 0.05%. Storage modulus (E'), loss modulus (E'') and $\tan \delta$ as a function of temperature at various frequencies were obtained from these runs. Data were the average of at least three samples.

RESULTS AND DISCUSSION

Time–Temperature Correspondence

The dynamic-mechanical storage moduli (E'), loss moduli (E''), and internal friction ($\tan \delta$) for water-blown rigid polyurethane foams containing 0 to 40% of SOYAFLUFF 200W at 4.5, 5.0, and 5.5% initial water content were measured at various temperatures and frequencies. Figure 1 showed

the results of storage moduli (E'), loss moduli (E''), and internal friction ($\tan \delta$) for control foam at 4.5% initial water content. All control and extended foams were very similar. The storage modulus increased with an increase of frequency and decreased with an increase of temperature. The maximum value of loss modulus near the glass transition region decreased and shifted to higher temperature with increasing frequency; the peak of internal friction also shifted to a higher temperature with an increase in frequency.

The glass transition temperature is an important indicator for applications of polymeric materials. The criterion for selection of glass transition temperature from DMA data is usually either the peak loss modulus, E'' , or peak $\tan \delta$. The peak $\tan \delta$ is the most prevalent criterion appearing in the literature because it corresponds more closely to the transition midpoint, while the peak loss modulus more closely denotes the initial drop from the glassy state into the transition.¹⁶ The glass transition temperature is dependent on the frequency;

Table II Properties of Water-Blown Rigid Polyurethane Foams Extended with SOYAFLUFF 200 W

Water Content, %	Biomass, %	Density, kg/m ³	Compressive Strength, kPa	Glass Transition Temperature, °C
4.5	0	33.8 ^a	218 ^{ab}	220.3 ^a
	10	34.1 ^a	234 ^b	223.2 ^a
	20	40.9 ^c	264 ^c	225.2 ^{ab}
	30	43.3 ^c	265 ^c	225.5 ^b
	40	45.2 ^c	244 ^c	229.5 ^c
5.0	0	32.1 ^a	202 ^a	223.8 ^{ab}
	10	32.5 ^a	217 ^{ab}	226.7 ^b
	20	34.9 ^{ab}	221 ^b	229.9 ^c
	30	40.4 ^{bc}	229 ^b	227.8 ^b
	40	41.5 ^c	234 ^b	229.5 ^c
5.5	0	30.5 ^a	186 ^a	227.0 ^b
	10	31.2 ^a	187 ^a	227.3 ^b
	20	34.8 ^{ab}	189 ^a	227.5 ^b
	30	36.2 ^b	200 ^a	229.4 ^c
	40	38.8 ^b	224 ^b	233.2 ^c

^{a,b,c} Means with the same letter in a column were not significantly different at the 5% level.

an increase in frequency usually leads to an increase in glass transition temperature. Traditionally, a frequency of 1 Hz has customarily been used as a standard value.¹⁶

Table II shows the glass transition temperature of the rigid polyurethane foams with 0 to 40% of SOYAFLUFF 200W at 4.5, 5.0, and 5.5% initial water content. The density and compressive strength from a previous study¹⁴ were also presented. As shown, the density, compressive strength, and glass transition temperature of extended foams were higher than those of control foams, and increased with increasing SOYAFLUFF 200W. The compressive strength of foams with and without SOYAFLUFF 200W also showed a similar trend. It appears that soy flour contributed to increases of both glass transition temperature and density, resulting in increased compressive strength.

Increasing the initial water content decreased both density and compressive strength, but increased the glass transition temperature. Increasing initial water content formed more urea bonds and less urethane bonds simultaneously in the rigid polyurethane foam system. Oertel¹⁷ reported that the urea bonds were more stable thermally (to 250°C) compared to the urethane bonds (to 180°C). Although the glass transition temperature increased with an increase of initial water content, the compressive strength decreased (Table II). This was probably because the effect of decreasing in foam density reduced the foam's compressive strength more than the effect of in-

creasing the glass transition temperature. Therefore, the glass transition temperature alone could not be used directly to predict the compressive strength of the low-density foams.

According to the time-temperature superposition principle (tTSP), it should be possible to construct a master curve from the data like E'' at different temperatures and frequencies. Figure 2 represents the master curves of the control foam at 4.5% initial water content. The plots of all control and extended foams were very similar. In all cases the temperature dependence of the shift factor along the frequency axis was illustrated according to the Williams-Landel-Ferry (WLF) equation

$$\log(a_T) = \frac{-C_1(T - T_0)}{C_2 + T - T_0} \quad (1)$$

where a_T is the temperature shift factor that is the ratio of a relaxation or retardation time at the chosen reference temperature, T_0 , to that at the temperature of measurement, T , and C_1 and C_2 are constants for a given polymer. The shape of these plots shows that the measured relaxation was not homogeneously broadened on the right side of the distribution. This could be the result of crystallinity or crosslinking of materials.¹² For rigid polyurethane foams with or without soy flour in this study, it was most likely a result of the crosslinking of materials. Table III summarizes the parameters for each of the foams with and without SOYAFLUFF 200W.

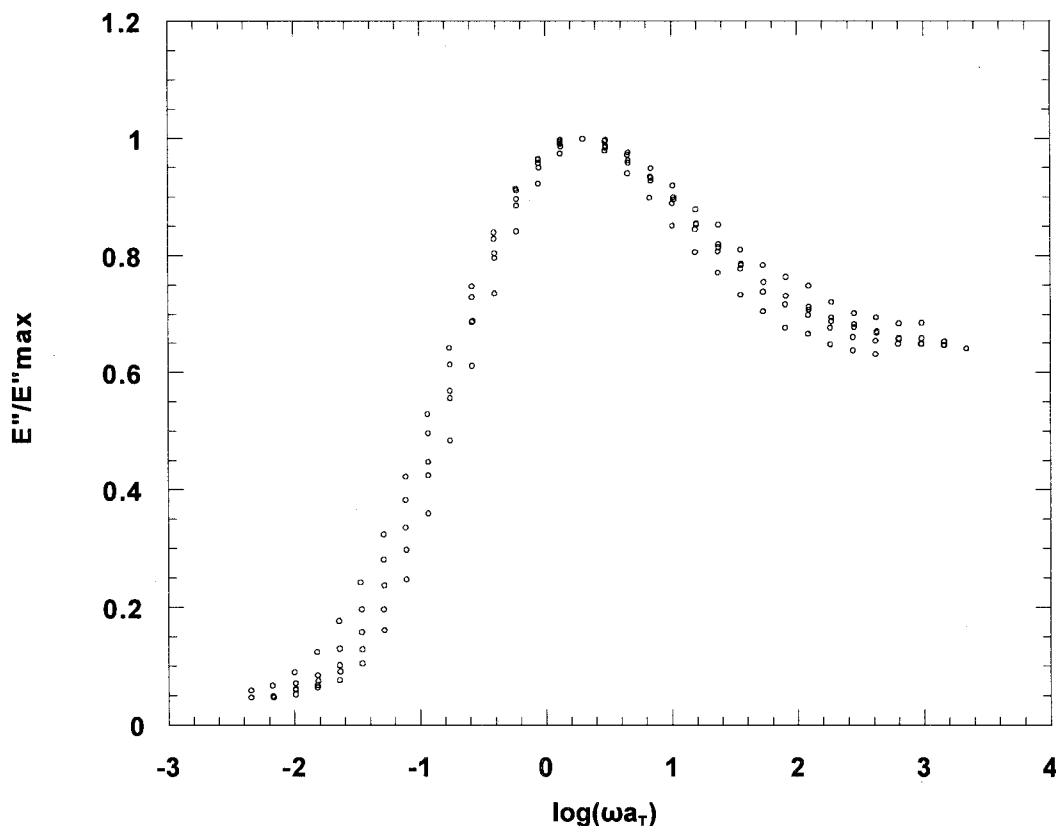


Figure 2 Master curve of the control foam at 4.5% initial water content.

Curve Fitting Using Theoretical Models

There are three popular empirical functions to describe the relaxation data of polymers in the

Table III Constants of Williams-Landel-Ferry Equation for the Foams With and Without SOYAFLUFF 200 W

Water Content, %	Biomass, %	C_1	$C_2, ^\circ\text{C}$
4.5	0	6.66	25.76
	10	7.30	32.84
	20	7.62	35.03
	30	7.96	39.98
	40	8.04	32.89
5.0	0	6.72	29.31
	10	7.32	32.09
	20	6.88	34.40
	30	7.54	39.79
5.5	40	7.87	37.33
	0	7.22	30.85
	10	7.50	33.00
	20	7.28	32.38
	30	7.82	37.41
	40	7.44	36.63

literature,^{5,18,19} such as Cole-Davison (CD), Kohlrausch-Williams-Watts (KWW), and Havriliak-Negami (HN) functions. Those functions were derived from experimental data of dielectric relaxation. There is a similar relaxation behavior that can be determined by three techniques: dielectric relaxation, photon correlation spectroscopy, and mechanical relaxation experiments.⁵ These functions also can be applied to describe the experimental data from photon correlation spectroscopy and mechanical relaxation experiments.

The normalized function is often equal to the measurements of the complex dielectric permittivity $E^*(\omega)$. The relationship is given as

$$\frac{E^*(\omega) - E_\infty}{E_0 - E_\infty} = E'(\omega) - iE''(\omega) \quad (2)$$

where $E'(4)$ and $E''(4)$ are the real and imaginary parts of the normalized dielectric permittivity, and E_0 and E_∞ are the limiting low- and high-frequency dielectric permittivities of the medium.¹⁹ According to a considerable amount of dielectric relaxation data, the empirical function is defined as

$$\frac{E^*(\omega) - E_\infty}{E_0 - E_\infty} \approx \left(\frac{1}{1 + i\omega\tau_{CD}} \right)^{\beta_{CD}} \quad (3)$$

where $0 < \beta_{CD} \leq 1$.²⁰

The dielectric permittivity is related to the relaxation function $\phi(t)$ by a one-sided Fourier or pure imaginary Laplace transform

$$\frac{E^*(\omega) - E_\infty}{E_0 - E_\infty} = \int_0^\infty \frac{d\phi(t)}{dt} \exp(-i\omega t) dt \quad (4)$$

where $\phi(t)$ is the relaxation function and ω is the frequency. Most data for a relevant relaxation function $\phi(t)$ fit the so-called Kohlrausch-Williams-Watts law

$$\phi(t) = A \exp[-(t/\tau_{KWW})^{\beta_{KWW}}] \quad (5)$$

A being a static correlation function and τ_{KWW} , a characteristic relaxation time. The exponent β_{KWW} ($0 < \beta_{KWW} \leq 1$) measures the departure from the Debye pure exponential law ($\beta_{KWW} = 1$). The average relaxation time is given as

$$\langle \tau \rangle = \tau_{KWW} \Gamma(\beta_{KWW}^{-1}) / \beta_{KWW} \quad (6)$$

where Γ is the gamma function.^{5,19}

The relaxation function of Havriliak and Negami²¹ successfully describes dielectric relaxation data near the glass transition. This function is

$$\frac{E^*(\omega) - E_\infty}{E_0 - E_\infty} = [1 + (i\omega\tau_{HN})^{1-\alpha}]^{-\beta_{HN}} \quad (7)$$

where τ_{HN} is a characteristic time of the relaxation process, and α and β_{HN} are empirical parameters that can range from 0 to 1.¹⁸

These functions include the real and imaginary parts. To fit these functions, it is necessary to separate the real and imaginary parts. For CD and HN functions, this may be accomplished by a successive application of DeMoivre's theorem to the denominator to extract the complex roots followed by a rationalization of the denominator. This procedure leads to the expression for CD function:²²

$$\frac{E'(\omega) - E_\infty}{E_0 - E_\infty} = (\cos \omega\tau_{CD})^{\beta_{CD}} \cos(\beta_{CD}\omega\tau_{CD}) \quad (8)$$

$$\frac{E''(\omega)}{E_0 - E_\infty} = (\cos \omega\tau_{CD})^{\beta_{CD}} \sin(\beta_{CD}\omega\tau_{CD}) \quad (9)$$

where E_0 and E_∞ are the values of the dielectric constant on the low- and high-frequency sides of the dispersion region, ω is the angular frequency, β_{CD} is the exponent that measures the departure from the Debye pure exponential form, and τ_{CD} is the relaxation time.

For HN function:²¹

$$\frac{E'(\omega) - E_\infty}{E_0 - E_\infty} = r^{-\beta_{HN}/2} \cos(\beta_{HN}\theta) \quad (10)$$

$$\frac{E''(\omega)}{E_0 - E_\infty} = r^{-\beta_{HN}/2} \sin(\beta_{HN}\theta) \quad (11)$$

with

$$r = [1 + (\omega\tau_{HN})^{1-\alpha} \sin \alpha(\pi/2)]^2 + [(\omega\tau_{HN})^{1-\alpha} \cos \alpha(\pi/2)]^2 \quad (12)$$

and

$$\theta = \tan^{-1} \left[\frac{(\omega\tau_{HN})^{1-\alpha} \cos \alpha(\pi/2)}{1 + (\omega\tau_{HN})^{1-\alpha} \sin \alpha(\pi/2)} \right] \quad (13)$$

where τ_{HN} is a characteristic time of the relaxation process, as well as α and β_{HN} are empirical parameters that can range from 0 to 1.

For analyzing KWW function in the frequency domain, a Fourier transform is needed. It is well known that there is no analytical expression for the Fourier transform of the KWW function. Several numerical methods^{19,23} have been used to obtain the Fourier transform of the KWW function and to interpret relaxation data from spectroscopies in the frequency domain. In this study, the following expression¹⁹ was used:

$$\begin{aligned} \frac{E^*(\omega) - E_\infty}{E_0 - E_\infty} &= \sum_{n=1}^{\infty} (-1)^{n-1} \frac{1}{(\omega\tau_{KWW})^{n\beta_{KWW}}} \times \frac{\Gamma(n\beta_{KWW} + 1)}{\Gamma(n + 1)} \\ &\times \left(\cos \beta_{KWW} \frac{n\pi}{2} - i \sin \beta_{KWW} \frac{n\pi}{2} \right). \quad (14) \end{aligned}$$

where τ_{KWW} is a characteristic relaxation time, and the exponent β_{KWW} ($0 < \beta_{KWW} \leq 1$) measures the departure from the Debye pure exponential law ($\beta_{KWW} = 1$). Both CD and KWW functions have two parameters. The β parameter in both functions determines the shapes of the function. β

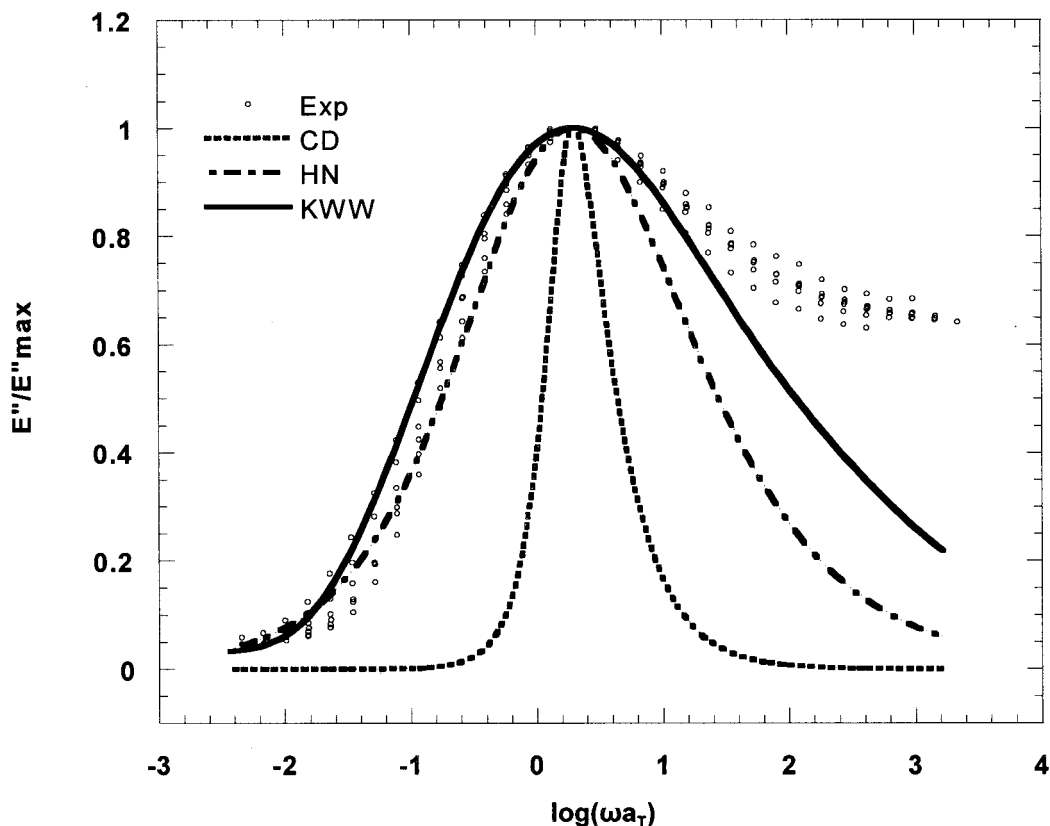


Figure 3 Comparison of the experimental master curve of E'' with those calculated with three different relaxation functions.

is referred to as a “width parameter”; as β becomes smaller, the distribution becomes broader. τ is a position parameter for the summit of the distribution function. In addition, HN function includes three parameters: α , β and τ . α and β control the width of the distribution function as well as β and τ contribute to the position of the summit of the distribution function.

It is possible to calculate the master curve through CD, HN, and KWW equations. Figure 3 shows the best fit to the master curve of the foam at 4.5% initial water content from these equations. The values of the parameters for these equations are shown in Table IV. According to the results of CD and KWW, there was no clear trend for β and τ , but most foams with SOYAFLUFF 200W had smaller β than control foam. Thus, most foams with biomass had a wider distribution function than control foams. Further research is needed to find whether a wider distribution function is indeed associated with observed increases in compressive strength and dimensional stability in the rigid polyurethane foams.^{13,14} Chartoff et al.¹⁶ reported that added particulate filler into the polymer system could widen the distribution

function. There was no clear trend for α , β , and τ , and it is difficult to find the relationship of parameters between HN and CD or KWW. In comparison, the HN function did not describe the master curves better than the KWW function for all foams, and the CD function resulted in master curves narrower than those from the HN or the KWW function.

Alvarez et al.²³ proposed a correlation between the parameter β of the KWW function and the parameters α and β of the HN function

$$\alpha\beta_{\text{HN}} = (\beta_{\text{KWW}})^{1.23} \quad (15)$$

When the parameters of Table IV were calculated by following this correlation function, the outcomes of Table V showed that the values of $\alpha\beta_{\text{HN}}$ and $(\beta_{\text{KWW}})^{1.23}$ are not similar. Hence, this relation did not hold satisfactorily. In addition, Lindsey and Patterson¹⁹ suggested a correlation between the parameters β and τ of the KWW and CD functions

$$\beta_{\text{KWW}} = \begin{cases} 0.970\beta_{\text{CD}} + 0.144, & 0.2 \leq \beta_{\text{CD}} \leq 0.6, \\ 0.683\beta_{\text{CD}} + 0.316, & 0.6 \leq \beta_{\text{CD}} \leq 1.0. \end{cases} \quad (16)$$

Table IV Parameters of the Konrausch-Williams-Watts, Havriliak-Negami, and Cole-Davidson Relaxation Function for the Foams With and Without SOYAFLUFF 200 W

Water Content, %	Biomass, %	KWW			HN			CD	
		β_{KWW}	τ_{KWW}	$\langle\tau_{KWW}\rangle$	α_{HN}	β_{HN}	τ_{HN}	β_{CD}	τ_{CD}
4.5	0	0.38	0.069	0.2360	0.493	0.800	0.550	0.243	0.259
	10	0.29	0.073	0.0026	0.497	0.709	0.850	0.151	0.458
	20	0.22	0.094	0.0026	0.582	0.933	0.769	0.078	1.229
	30	0.20	0.053	0.0012	0.570	0.754	0.701	0.055	1.004
	40	0.21	0.078	0.0019	0.538	0.852	0.655	0.068	1.207
5.0	0	0.27	0.071	0.0377	0.556	0.783	0.788	0.135	0.523
	10	0.30	0.083	0.0869	0.513	0.832	0.859	0.165	0.485
	20	0.26	0.054	0.0022	0.527	0.730	0.625	0.120	0.509
	30	0.24	0.084	0.0027	0.546	0.892	0.858	0.102	0.839
	40	0.20	0.089	0.0020	0.586	0.948	0.920	0.058	1.686
5.5	0	0.30	0.074	0.0775	0.499	0.715	0.743	0.162	0.432
	10	0.20	0.087	0.0019	0.563	0.907	0.750	0.056	1.648
	20	0.21	0.072	0.0018	0.532	0.789	0.780	0.069	1.114
	30	0.21	0.050	0.0012	0.523	0.682	0.455	0.071	0.774
	40	0.20	0.068	0.0015	0.552	0.800	0.544	0.057	1.288

The parameters obtained for the CD function satisfied quite well the relations with the β and τ of the KWW function (Table VI).

CONCLUSIONS

The addition of soy flour in the rigid polyurethane foam system contributed to a higher glass transition temperature. Also, increasing initial water

content resulted in an increase of the glass transition temperature. The compressive strength of rigid polyurethane foam could not be predicted by the data of glass transition temperature. Moreover, the master curves for all foams were successfully constructed through the WLF equation according to the time-temperature superposition principle. The results from the master curves showed that most foams with biomass had a wider relaxation distribution than the control

Table V Comparison of Values from $(\beta_{KWW})^{1,23}$ and $\alpha\beta_{HN}$ for the Foams With and Without SOYAFLUFF 200 W

Water Content, %	Biomass, %	$(\beta_{KWW})^{1,23}$	$\alpha\beta_{HN}$
4.5	0	0.304	0.394
	10	0.278	0.352
	20	0.155	0.543
	30	0.138	0.430
	40	0.147	0.458
5.0	0	0.200	0.435
	10	0.227	0.427
	20	0.191	0.385
	30	0.173	0.487
	40	0.138	0.556
5.5	0	0.227	0.357
	10	0.138	0.511
	20	0.147	0.420
	30	0.147	0.357
	40	0.138	0.442

Table VI Comparison of Values of β_{KWW} and Calculated β_{KWW} for the Foams With and Without SOYAFLUFF 200 W

Water Content, %	Biomass, %	β_{KWW}	β_{KWW} (cal)
4.5	0	0.38	0.379
	10	0.29	0.291
	20	0.22	0.220
	30	0.20	0.197
	40	0.21	0.210
5.0	0	0.27	0.275
	10	0.30	0.304
	20	0.26	0.260
	30	0.24	0.243
	40	0.20	0.200
5.5	0	0.30	0.301
	10	0.20	0.198
	20	0.21	0.211
	30	0.21	0.213
	40	0.20	0.199

foams. The KWW function fit the master curve better than the HN and CD functions.

This article was a contribution from the Missouri Agricultural Experiment Station, Journal Series No. 12,994.

REFERENCES

1. Woods, G. *The ICI Polyurethanes Book*; John Wiley & Sons: New York, 1990, 2nd ed.
2. Wirpsza, Z. *Polyurethanes: Chemistry, Technology, and Applications*; Ellis Horwood: New York, 1993.
3. Goldstein, M.; Simha, R., Eds. *The Glass Transition and the Nature of the Glassy State*; New York Academy of Sciences: New York, 1976.
4. Jäckle, J. *Rep Prog Phys* 1986, 49, 171.
5. Sanchís, A.; Prolongo, M. G.; Masegosa, R. M.; Rubio, R. G. *Macromolecules* 1995, 28, 2693.
6. Ngai, K. L.; Rendell, R. W. *J Mol Liq* 1993, 56, 199.
7. Götze, W.; Sjögren, L. *Rep Prog Phys* 1992, 55, 241.
8. Götze, W.; Sjögren, L. *J Non-Cryst Solids* 1991, 131–133, 153.
9. Götze, W.; Sjögren, L. *J Non-Cryst Solids* 1991, 131–133, 161.
10. Li, G.; Du, W. M.; Chen, X. K.; Cummins, H. Z.; Tao, N. J. *Phys Rev A* 1992, 45, 3867.
11. Santangelo, P. G.; Ngai, K. L.; Roland, C. M. *Macromolecules* 1994, 27, 3859.
12. Roland, C. M.; Santangelo, P. G.; Baram, Z.; Runt, J. *Macromolecules* 1994, 27, 5382.
13. Lin, Y.; Hsieh, F.; Huff, H. E.; Iannotti, E. *Cereal Chem* 1996, 73, 189.
14. Chang, L.; Xue, Y.; Hsieh, F. *J Appl Polym Sci*, to appear.
15. Bailey, F. E.; Critchfield, F. E. *J Cell Plast* 1981, 17, 333.
16. Chartoff, R. P.; Weissman, P. T.; Sircar, A. In *Assignment of the Glass Transition*; ASTM: Philadelphia, 1994.
17. Oertel, G. *Polyurethane Handbook*; Hanser Verlag: Munich, 1993, 2nd ed.
18. Alberdi, J. M.; Alvarez, F.; Alegría, A.; Colmenero, J. In *Basic Features of the Glassy State*; World Scientific: Singapore, 1989.
19. Lindsey, C. P.; Patterson, G. D. *J Chem Phys* 1980, 73, 3348.
20. Davidson, D. W.; Cole, R. H. *J Chem Phys* 1951, 19, 1484.
21. Havrilliak, S.; Negami, S. *J Polym Sci Part C* 1966, 14, 99.
22. Davidson, D. W. *Can J Chem* 1961, 39, 571.
23. Alvarez, F.; Alegría, A.; Colmenero, J. *Phys Rev B* 1991, 44, 7306.